Sensor-based Simultaneous Localization and Mapping – Part II: Online Inertial Map and Trajectory Estimation

Bruno J. Guerreiro, Pedro Batista, Carlos Silvestre, and Paulo Oliveira

***Abstract*— A novel sensor-based filter for simultaneous localization and mapping (SLAM), featuring globally asymptotically stable error dynamics, is proposed in a companion paper, with application to uninhabited aerial vehicles (UAVs). This paper presents the second part of the algorithm, detailing a computationally efficient and numerically robust method for online inertial map and trajectory estimation based on the estimates provided by the SLAM filter previously derived. Central to the solution is the formulation of an optimization problem, that of finding the translation and the rotation that best explain the transformation between two sets of landmarks, with known associations, for consecutive time instants. The validation, performance, and consistency assessment of the proposed SLAM algorithm is successfully performed with real data, which was acquired by an instrumented quadrotor.**

I. Introduction

Recently, the automatic inspection of critical infrastructures and buildings, such as bridges, electric power lines, dams, and construction areas, has been acknowledged as a challenging and promising application scenario for the use of uninhabited aerial vehicles (UAVs). Near these structures, the position measured by a global positioning system (GPS) can degrade severely and the magnetic field is locally distorted, precluding the use of magnetometers. The use of aided navigation techniques, as proposed in this work using a SLAM algorithm, aims at solving this problem without using these, possibly compromised, sensing devices.

In the companion paper [1] a globally asymptotically stable (GAS) sensor-based SLAM navigation filter is proposed, with application to UAVs in GPS-denied environments, and considering acceleration and angular rate inertial measurements, as well as ranging measurements provided by a LASER scanning device and an altitude sensor. A detailed survey and tutorial on SLAM techniques can be found in [2], [3], and references therein. One of the most successful strategies is to use the discrete-time EKF-SLAM algorithm, considering the full state to be composed of the vehicle pose and the location of all the map landmarks described in the inertial frame, and estimated at each iteration based on the open-loop prediction and the matched landmark observations. Conversely, the SLAM filter proposed in the companion paper [1] represents all landmark positions in the vehicle/sensor coordinate frame, making the positioning of the vehicle in the map trivial (i.e. at the origin and aligned with the sensor frame) and consequently, not included in the state vector.

This paper proposes an algorithm to compute the optimal transformation that enables the estimation of the inertial map and vehicle trajectory using the sensor-based map provided by the SLAM filter. This is achieved by estimating the translation and rotation between two instants, provided at least two successful landmark associations between them. Thus, with the knowledge of the vehicle pose at the initialization instant, usually considered to be the inertial frame, it is possible to incrementally map the sensor-based quantities into the inertial frame. The problem of extracting the orthogonal transformation that maps one set of known points into a second set of known points, with known associations between them, can be rewritten by subtracting the centroid of each point set, resulting in the problem of finding solely the rotation matrix between the modified sets, as in [4], [5]. This is usually called the generalized orthogonal Procrustes problem [6] and has a closed-form solution directly computed in the space of the special orthogonal matrices, as derived in [5]. The main contributions of this paper are: (i) the formulation and closed-form solution for the problem of obtaining the transformation from the sensor frame to inertial frame; (ii) the formulation of the traditional body to inertial transformation solution, based on state augmentation, and comparison with the closed-form solution; and (iii) the detailed presentation and discussion of the proposed SLAM algorithm results, both in the body and inertial frames.

The paper is organized as follows. Section II presents a brief description of the sensor-based filter derived in the companion paper [1] and additional features that can be easily incorporated in the filter design are discussed. An example is provided with direction measurements associated with each landmark. Section III introduces the problem addressed in this paper and Section IV provides a closed-form optimal solution. Experimental results are shown and discussed in Section V and, finally, Section VI gives some concluding remarks and directions for future work.

Throughout the paper the symbol $\mathbf{0}_{n\times m}$ denotes an $n \times m$ matrix of zeros, $\mathbf{I}_n$ an identity matrix with dimension $n \times n$, and $\mathrm{diag}(\mathbf{A}_1, \ldots, \mathbf{A}_\mathrm{n})$ a block diagonal matrix. When the dimensions are omitted the matrices are assumed of appropriate dimensions.

This work was partially supported by project FCT [PEst-OE/EEI/LA0009/2011], by project FCT AMMAIA (PTDC/HIS-ARQ/103227/2008), and by project AIRTICI from AdI through the POS Conhecimento Program that includes FEDER funds. The work of Bruno Guerreiro was supported by the PhD Student Grant SFRH/BD/21781/2005 from the Portuguese FCT POCTI programme.

B. J. Guerreiro, P. Batista, C. Silvestre, and Paulo Oliveira are with the Institute for Systems and Robotics, Instituto Superior Técnico, at the Technical University of Lisbon, Av. Rovisco Pais 1, 1049-001 Lisboa, Portugal. C. Silvestre is also with the Faculty of Science and Technology, University of Macau, Taipa, Macau.
{bguerreiro,pbatista,cjs,pjcro}@isr.ist.utl.pt

II. Brief Overview

In this section the filter presented in the companion paper [1], is briefly described. Moreover, it is also shown that additional features can be easily incorporated in the filter design, namely with an example where directions associated with a landmark are considered.

A. Sensor-based Dynamics

Let $\{I\}$ denote the local inertial frame, $\{H\}$ the horizontally projected body-fixed frame, hereafter referred to as just the sensor frame, and ${}^{I}_{H}\mathbf{R}(t) \in \mathrm{SO}(2)$ the rotation matrix from $\{H\}$ to $\{I\}$. For the sake of simplicity, these frames and their related variables are considered to be in 2-dimensional (2-D) space, unless otherwise stated. Let also ${}^{I}\mathbf{p}_{H}(t) \in \mathbb{R}^2$ denote the position of the origin of $\{H\}$, described in $\{I\}$, and $\mathbf{v}(t) \in \mathbb{R}^2$ the velocity of the vehicle relative to $\{I\}$, expressed in $\{H\}$. The linear motion kinematics of the vehicle are given by ${}^{I}\dot{\mathbf{p}}_{H}(t) = {}^{I}_{H}\mathbf{R}(t)\,\mathbf{v}(t)$, while the angular motion kinematics satisfy ${}^{I}_{H}\dot{\mathbf{R}}(t) = {}^{I}_{H}\mathbf{R}(t)\,\mathbf{S}\,r(t)$, where $r(t) \in \mathbb{R}$ is the angular velocity of the vehicle expressed in $\{H\}$, and $\mathbf{S} = \begin{bmatrix} 0 & -1 \\ 1 & 0 \end{bmatrix}$ is a skew-symmetric matrix.

Considering a LASER scanner mounted horizontally in the vehicle, so that the measurements projected into $\{H\}$ represent a horizontal profile of the environment, and an altitude sensor, either a SONAR or a LASER range finder, the complete 3-dimensional (3-D) position and a 2-dimensional (2-D) map of the environment can be obtained using a SLAM algorithm. The underlying standard assumption is that the environment is fairly structured in altitude. Each detected landmark can be represented by a 2-D position and, optionally, one or two 2-D vectors representing directions, and other constant parameters. A corner, even if only partially visible, is a very informative landmark that can provide a measure of position as well as one or two measures of attitude, given by the direction of each wall. For this reason, the landmark formulation, presented in the companion paper [1], is further extended to include directions. Considering the case of a single direction associated with a landmark, since the extention to more directions is trivial, the position and the direction associated with the i-th landmark expressed in $\{H\}$, denoted by $\mathbf{p}_i \in \mathbb{R}^2$ and $\mathbf{d}_i \in \mathbb{R}^2$, respectively, satisfy

$$\begin{cases} \mathbf{p}_i(t) = {}^{I}_{H}\mathbf{R}^T(t)\,({}^{I}\mathbf{p}_i - {}^{I}\mathbf{p}_H(t)) \\ \mathbf{d}_i(t) = {}^{I}_{H}\mathbf{R}^T(t)\,{}^{I}\mathbf{d}_i \end{cases},$$

where ${}^{I}\mathbf{p}_i \in \mathbb{R}^2$ and ${}^{I}\mathbf{d}_i \in \mathbb{R}^2$ denote the static inertial 2-D position and direction associated with the landmark. In the sensor-based framework, their kinematics can be written as

$$\begin{cases} \dot{\mathbf{p}}_i(t) = -\left[r_m(t) - b_r(t)\right]\,\mathbf{S}\,\mathbf{p}_i(t) - \mathbf{v}(t) \\ \dot{\mathbf{d}}_i(t) = -\left[r_m(t) - b_r(t)\right]\,\mathbf{S}\,\mathbf{d}_i(t) \end{cases},$$

where $r_m(t)$ denotes the angular velocity measurement and $b_r(t)$ the respective bias. In a SLAM state-space formulation, the full stochastic state vector, here denoted as $\mathbf{x}_F \in \mathbb{R}^{n_{x_F}}$, can be decomposed into vehicle specific variables, $\mathbf{x}_V \in \mathbb{R}^{n_{x_V}}$, and landmark variables, $\mathbf{x}_M \in \mathbb{R}^{n_{x_M}}$. In the proposed formulation, the vehicle state vector is formed by the altitude $z(t) \in \mathbb{R}$, the linear velocity in $\{H\}$, $\mathbf{v}(t) \in \mathbb{R}^2$, the vertical velocity $v_z(t) \in \mathbb{R}$, and the bias of the angular velocity measurement in $\{H\}$, $b_r(t) \in \mathbb{R}$, yielding $\mathbf{x}_V(t) = \begin{bmatrix} z(t) & \mathbf{v}(t) & v_z(t) & b_r(t) \end{bmatrix}^T$. A further decomposition of the landmark state-space into observed and unobserved landmarks is considered, for the sake of clarity, such that $\mathbf{x}_M = \begin{bmatrix} \mathbf{x}_{MO}^T & \mathbf{x}_{MU}^T \end{bmatrix}^T$, where $\mathbf{x}_{MO} = \{\mathbf{m}_i\} \in \mathbb{R}^{n_{x_m}}$, for all $i \in \mathcal{I}_O = \{o_1, \ldots, o_{no}\}$, and $\mathbf{x}_{MU} = \{\mathbf{m}_i\} \in \mathbb{R}^{n_{x_{MU}}}$, for all $i \in \mathcal{I}_U$. Note that the union of the sets of observed and unobserved landmarks, $\mathcal{I}_O$ and $\mathcal{I}_U$, respectively, yields $\mathcal{I} = \mathcal{I}_O \cup \mathcal{I}_U = \{1, \ldots, n_M\}$. The landmark vector $\mathbf{m}_i$ can feature the position of the landmark and up to two directions, e. g. to represent a corner landmark would yield $\mathbf{m}_i = \begin{bmatrix} \mathbf{p}_i^T & \mathbf{d}_{1_i} & \mathbf{d}_{2_i} \end{bmatrix}^T$.

With the above introduction and considering that the linear velocities are slowly time-varying, the complete system dynamics in $\{H\}$ can now be written as

$$\begin{cases} \dot{\mathbf{x}}_V(t) = \mathbf{A}_V\,\mathbf{x}_V(t) \\ \dot{\mathbf{m}}_i(t) = \mathbf{A}_{MV_i}(\mathbf{m}_i(t))\mathbf{x}_V(t) + \mathbf{A}_{M_i}(t)\mathbf{m}_i(t)\,\forall_{i\in\mathcal{I}} \\ y_z(t) = \mathbf{C}_z\,\mathbf{x}_V(t) \\ \mathbf{y}_{MO}(t) = \mathbf{x}_{MO}(t) \end{cases}, \quad (1)$$

where, considering landmarks with only one direction, it is a matter of algebraic manipulation to obtain

$$\mathbf{A}_V = \begin{bmatrix} 0 & \mathbf{0}_{1\times 2} & -1 & 0 \\ \mathbf{0}_{2\times 1} & \mathbf{0}_{2\times 2} & \mathbf{0}_{2\times 1} & \mathbf{0}_{2\times 1} \\ 0 & \mathbf{0}_{1\times 2} & 0 & 0 \\ 0 & \mathbf{0}_{1\times 2} & 0 & 0 \end{bmatrix},$$

$$\mathbf{A}_{MV_i}(\mathbf{m}_i(t)) = \begin{bmatrix} \mathbf{0}_{2\times 1} & -\mathbf{I}_2 & \mathbf{0}_{2\times 1} & \mathbf{S}\,\mathbf{p}_i(t) \\ \mathbf{0}_{2\times 1} & \mathbf{0}_{2\times 2} & \mathbf{0}_{2\times 1} & \mathbf{S}\,\mathbf{d}_i(t) \end{bmatrix},$$

where $\mathbf{A}_{M_i}(t) = -r_m(t)\,\mathbf{S}_2$ and $\mathbf{C}_z = \begin{bmatrix} 1 & \mathbf{0}_{1\times(n_{x_V}-1)} \end{bmatrix}$, denoting $\mathbf{S}_n$ as the block diagonal matrix formed using n times the matrix $\mathbf{S}$, in this case $\mathbf{S}_2 = \mathrm{diag}\,(\mathbf{S}, \mathbf{S})$. The extension to more than one direction associated with a landmark is trivial, and therefore is omitted.

B. SLAM Filter

In a SLAM filter, the observed landmarks are a subset of the state landmarks, whereas the unobserved landmarks are integrated in open-loop. For filter design purposes, the unobserved landmarks are not considered, leading to the reduced state-space vector $\mathbf{x} = \begin{bmatrix} \mathbf{x}_V^T & \mathbf{x}_{MO}^T \end{bmatrix}^T \in \mathbb{R}^{n_x}$ and output vector $\mathbf{y} = \begin{bmatrix} y_z & \mathbf{y}_{MO}^T \end{bmatrix}^T \in \mathbb{R}^{n_y}$. Thus, it is straightforward to rewrite (1) as

$$\begin{cases} \dot{\mathbf{x}}(t) &= \mathbf{A}(t)\,\mathbf{x}(t) \\ \mathbf{y}(t) &= \mathbf{C}\,\mathbf{x}(t) \end{cases}, \quad (2)$$

where

$$\mathbf{A}(t) = \begin{bmatrix} \mathbf{A}_v & \mathbf{0}_{n_{x_v}\times n_{x_m}} \\ \mathbf{A}_{MV}(t) & \mathbf{A}_M(t) \end{bmatrix},$$

$$\mathbf{A}_{MV}(t) = \begin{bmatrix} \mathbf{A}_{MV_{o_1}}^T(t) & \ldots & \mathbf{A}_{MV_{o_{no}}}^T(t) \end{bmatrix}^T,$$

$$\mathbf{A}_{MV_i}(t) = \mathbf{A}_{MV_i}(\mathbf{m}_{i_m}(t))\,\forall_{i\in\mathcal{I}_O},$$

$$\mathbf{A}_M(t) = \mathrm{diag}\left(\mathbf{A}_{M_{o_1}}(t), \ldots, \mathbf{A}_{M_{o_{no}}}(t)\right), \text{ and}$$

$$\mathbf{C} = \begin{bmatrix} \mathbf{C}_z & \mathbf{0}_{1\times n_{x_{MO}}} \\ \mathbf{0}_{n_{x_{MO}}\times n_{x_V}} & \mathbf{I}_{n_{x_{MO}}} \end{bmatrix} .$$

As mentioned in the companion paper [1], the dynamic system (1) is nonlinear. However, written in the form (2), it can be regarded as a linear time-varying system for observer design purposes, as the system matrix $\mathbf{A}(t)$ may be written in such a way that it does not depend on the state, which is estimated, but on the actual output, which is measured and readily available. This approach has been successfully employed by the authors, see e.g. [7].

The implementation of a SLAM filter for (1) follows naturally with a discrete Kalman filter, as all the sensors and the processing units are sample-based. Thus, using the sample notation $\mathbf{x}_k := \mathbf{x}(t_k)$, with $t_k = k\,T_s + t_0$, $k \in \mathbb{N}_0$ and t_0 as the initial time, the Euler discretization of the system dynamics (2) with system disturbance, $\mathbf{w}_k$, and measurement noise, $\mathbf{n}_{k+1}$, yields

$$\begin{cases} \mathbf{x}_{k+1} = \mathbf{F}_k\,\mathbf{x}_k + \mathbf{w}_k \\ \mathbf{y}_{k+1} = \mathbf{H}_{k+1}\,\mathbf{x}_{k+1} + \mathbf{n}_{k+1} \end{cases} , \tag{3}$$

where $\mathbf{F}_k = \mathbf{I}_{n_x} + T_s\,\mathbf{A}_k$, $\mathbf{H}_k = \mathbf{C}_k$, $\mathbf{w}_k \in \mathbb{R}^{n_x}$ and $\mathbf{n}_k \in \mathbb{R}^{n_y}$ are zero-mean discrete white Gaussian noise, with $E[\mathbf{w}_k\,\mathbf{w}_l^T] = \mathbf{Q}_k\,\delta_{k-l}$ and $E[\mathbf{n}_k\,\mathbf{n}_l^T] = \mathbf{R}_k\,\delta_{k-l}$, respectively, and δ_k denotes the Dirac delta function. The resulting discrete Kalman filter equations for the above system are standard [8], [9]. Nonetheless, system (3) does not account for the unobserved landmarks $\mathbf{x}_{MU}$, which have to be propagated in open-loop using a discrete version of the equations defined in (1). Using the full system state vector $\mathbf{x}_F = \begin{bmatrix}\mathbf{x}^T & \mathbf{x}_{MU}^T\end{bmatrix}^T$, the complete filter, described in the first part of this work, [1], provides at each sampling instant the estimated state $\hat{\mathbf{x}}_{F_{k|k}}$ and respective covariance matrix $\mathbf{P}_{F_{k|k}}$, which can be decomposed as

$$\mathbf{P}_{F_{k|k}} = \begin{bmatrix} \mathbf{P}_{V_{k|k}} & \mathbf{P}_{VM_{k|k}} \\ \mathbf{P}_{VM_{k|k}}^T & \mathbf{P}_{M_{k|k}} \end{bmatrix} ,$$

where $\mathbf{P}_{M_{k|k}} = \left\{\mathbf{P}_{\mathbf{m}_i\mathbf{m}_j\,k|k}\right\}$ for all $i, j \in \mathcal{I}$. The next section formulates the problem of finding the transformation from the sensor-frame $\{H\}$ to the inertial frame $\{I\}$, or equivalently, finding the position and orientation of the vehicle in $\{I\}$, given the filter estimates.

III. Problem Formulation

The transformation from the reference frame $\{H\}$ to the reference frame $\{I\}$, at a given instant k, is defined by the position and orientation of the vehicle in $\{I\}$, given by ${}^I\mathbf{p}_{H_k} \in \mathbb{R}^2$ and ${}^I_H\mathbf{R}_k \in \mathrm{SO(2)}$, respectively. The objective of this section is to formulate the underlying optimization problem to obtain these quantities, so that it is possible to generate not only the inertial trajectory of the vehicle but also the inertial positions of the landmarks.

Without loss of generality, assume that the inertial frame is coincident with the vehicle pose, at the algorithm initialization instant k_0, that is, ${}^I\mathbf{p}_{H_{k_0}} = \mathbf{0}_{2\times 1}$ and ${}^I_H\mathbf{R}_{k_0} = \mathbf{I}_2$, and, consequently, all landmarks and respective directions are given by ${}^I\mathbf{p}_{i_{k_0}} = {}^H\mathbf{p}_{i_{k_0}}$ and ${}^I\mathbf{d}_{i_{k_0}} = {}^H\mathbf{d}_{i_{k_0}}$ for all $i \in \mathcal{I}_{k_0}$. Further assume that the relations between time samples of the inertial positions of the vehicle frame and the landmarks satisfy

$$\begin{cases} {}^I\mathbf{p}_{H_k} = {}^I\mathbf{p}_{H_{k-1}} + {}^I\delta\mathbf{p}_{H_k} \\ {}^I\mathbf{p}_{i_k} = {}^I\mathbf{p}_{i_{k-1}} \end{cases} , \tag{4}$$

where ${}^I\delta\mathbf{p}_{H_k} \in \mathbb{R}^2$ represents the translation of the position of the vehicle between the sampling time $k-1$ and the sampling time k. The rotation matrix satisfies

$${}^I_H\mathbf{R}_k = {}^I_H\mathbf{R}_{k-1}\,{}^I_H\delta\mathbf{R}_k, \tag{5}$$

where ${}^I_H\delta\mathbf{R}_k \in \mathrm{SO(2)}$ is the rotation matrix that represents the change of orientation of the vehicle between the sampling time $k-1$ and the sampling time k. The idea is to express the known landmark position in the sensor frame at a given instant k as a function of the landmark position in the same frame at the previous instant $k-1$, which is also available, and using (4) and (5) this can be written as

$$\begin{aligned} \mathbf{p}_{i_k} &= {}^I_H\mathbf{R}_k^T\left[{}^I\mathbf{p}_{i_k} - {}^I\mathbf{p}_{H_k}\right] \\ &= {}^I_H\delta\mathbf{R}_k^T\,\mathbf{p}_{i_{k-1}} - {}^I_H\delta\mathbf{R}_k^T\,{}^I_H\mathbf{R}_{k-1}^T\,{}^I\delta\mathbf{p}_{H_k} . \end{aligned} \tag{6}$$

For the sake of simplicity of notation, let $\delta\mathbf{R}_k := {}^I_H\delta\mathbf{R}_k^T$ and $\delta\mathbf{p}_k := -{}^I_H\delta\mathbf{R}_k^T\,{}^I_H\mathbf{R}_{k-1}^T\,{}^I\delta\mathbf{p}_{H_k}$. Then, (6) can simply be stated as

$$\mathbf{p}_{i_k} = \delta\mathbf{R}_k\,\mathbf{p}_{i_{k-1}} + \delta\mathbf{p}_k .$$

Therefore, defining the error function

$$\mathbf{e}_{i_k} = \mathbf{p}_{i_k} - \delta\mathbf{R}_k\,\mathbf{p}_{i_{k-1}} - \delta\mathbf{p}_k,$$

the transition transformation from instant $k-1$ to k, denoted as the pair $(\delta\mathbf{R}_k, \delta\mathbf{p}_k)$, can be found by solving the optimization problem

$$(\delta\mathbf{R}_k^*, \delta\mathbf{p}_k^*) = \arg \min_{\substack{\delta\mathbf{R}_k \in \mathrm{SO(2)} \\ \delta\mathbf{p}_k \in \mathbb{R}^2}} \frac{1}{n_{\delta_k}} \sum_{i\in\mathcal{I}_{\delta_k}} \mathbf{e}_{i_k}^T\,\mathbf{e}_{i_k} , \tag{7}$$

where the set of the landmarks used to find this transformation is denoted as $\mathcal{I}_{\delta_k} = \{\delta_1, \ldots, \delta_{n_{\delta_k}}\}$, obtained from the sensor-based filter proposed in the companion paper [1].

IV. Inertial Map and Trajectory Estimation

A. Closed-form solution

The optimization problem (7) defined in the previous section has a closed-form, computationally efficient, and numerically robust solution. In [5], the problem of computing the translation, rotation and scaling parameters between two clouds of 3-D points with known one-to-one point associations is solved, resorting to the singular value decomposition SVD algorithm to find the rotation matrix component of the solution. In the particular case discussed in this paper, the two clouds of 2-D points are given by $\mathbf{p}_{i_k}\forall_{i\in\mathcal{I}_{\delta_k}}$ and $\mathbf{p}_{i_{k-1}}\forall_{i\in\mathcal{I}_{\delta_k}}$, and it is assumed that there is no scaling between them.

The idea behind the closed-form solution arising from this type of problems is to find the centroids of each cloud of points, given by

$$\boldsymbol{\mu}_k = \frac{1}{n_{\delta_k}} \sum_{i\in\mathcal{I}_{\delta_k}} \mathbf{p}_{i_k} \quad \text{and} \quad \boldsymbol{\mu}_{k-1} = \frac{1}{n_{\delta_k}} \sum_{i\in\mathcal{I}_{\delta_k}} \mathbf{p}_{i_{k-1}} ,$$

enabling the computation of the rotation matrix that best explains the rotation between the two centered clouds of points, which results from the SVD of the matrix

$$\mathbf{\Sigma}_{k,k-1} = \frac{1}{n_{\delta_k}} \sum_{i \in \mathcal{I}_{\delta_k}} \left(\mathbf{p}_{i_k} - \boldsymbol{\mu}_k\right) \left(\mathbf{p}_{i_{k-1}} - \boldsymbol{\mu}_{k-1}\right)^T ,$$

which is defined as $\text{svd}\left(\mathbf{\Sigma}_{k,k-1}\right) = \mathbf{U}_k \, \mathbf{D}_k \, \mathbf{V}_k^T$. The rotation matrix in SO(2) is then naturally found using the expression

$$\delta\mathbf{R}_k^* = \mathbf{U}_k \, \mathbf{S}_k \, \mathbf{V}_k^T ,$$

where the diagonal matrix $\mathbf{S}_k$ is defined as $\mathbf{S}_k = \text{diag}(1, \det(\mathbf{U}_k)\det(\mathbf{V}_k))$. With the optimal rotation matrix found, the translation term is readily given by

$$\delta\mathbf{p}_k^* = \boldsymbol{\mu}_k - \delta\mathbf{R}_k^* \, \boldsymbol{\mu}_{k-1} .$$

With the closed-form solution of the optimization problem (7), it is trivial to compute the pose of the vehicle at each instant based on the previous pose, which is simply obtained from

$$\begin{cases} {}^I_H\mathbf{R}_k = {}^I_H\mathbf{R}_{k-1} \, \delta\mathbf{R}_k^{*T} , \\ {}^I\mathbf{p}_{H_k} = {}^I\mathbf{p}_{H_{k-1}} - {}^I_H\mathbf{R}_{k-1} \, \delta\mathbf{R}_k^{*T} \, \delta\mathbf{p}_k^* . \end{cases} \tag{8}$$

With (8), all the variables provided by the filter, expressed in the sensor frame, can be transformed into the inertial frame. Thus, the inertial estimates of the i-th landmark, considering also one direction as part of the landmark, are given by

$$\begin{cases} {}^I\mathbf{p}_{i_k} = {}^I_H\mathbf{R}_k \mathbf{p}_{i_k} + {}^I\mathbf{p}_{H_k} , \\ {}^I\mathbf{d}_{i_k} = {}^I_H\mathbf{R}_k \mathbf{d}_{i_k} . \end{cases}$$

Remark 1: The estimation uncertainty of the transformation is not presented in this paper and it will be addressed in future work. The aim will be, under some realistic assumptions, to find approximate estimates for the covariance matrices of the inertial-based trajectory and map, provided the uncertainty estimates of the transformation resulting from the solution of (7).

B. Alternative Approach

In a similar fashion to the approach presented in [10], an alternative approach is to include the inertial frame in the sensor-based SLAM filter by augmenting the state with its position and orientation, which will always be unobservable. In the SLAM formulation presented in this work the inclusion of the position is trivial and can be seen as a point landmark, denoted here by $\mathbf{p}_{0_k}$. As for the orientation, the state can be augmented to include an angle representing the relative orientation of the inertial frame in the sensor frame, ψ_{0_k}. The values used for initialization at instant k_0 are $\mathbf{p}_{0_{k_0}} = \mathbf{0}_{2\times 1}$ and $\psi_{0_{k_0}} = 0$, noting that the motion kinematics of the angle approach, which was not introduced before, is given by $\dot{\psi}_0(t) = -r_m(t) + b_r(t)$. Thus, one can trivially obtain the rotation matrix by using ${}^I_H\mathbf{R}_k = \mathbf{R}_{\psi_{0_k}}$, which denotes the 2-D rotation of an angle ψ_{0_k}, and afterwards the position of the sensor-frame described in the inertial frame as ${}^I\mathbf{p}_{H_k} = -{}^I_H\mathbf{R}_k \, \mathbf{p}_{0_{k_0}}$.

V. Experimental Results

This section describes the experimental setup and presents the results for the proposed overall sensor-based SLAM algorithm. While the results presented in the first part of this work, [1], focused on the filter convergence properties, in this section the consistency of the algorithm, the ability to close a 60 meter loop, and the inertial map and trajectory estimation results are discussed.

An instrumented quadrotor was hand-driven along a path of about 60 meters in an indoor environment with a loop, as shown in Fig. 1, at an average speed of 0.4 m/s. The trajectory described by the vehicle starts near the middle and circulates counter clockwise until some of the first landmaks detected are once again visible (at the lower right corner). This custom quadrotor UAV, property of ISR, is equipped with a MEMSENS nanoIMU, a Maxbotix XL SONAR for altitude measurements, and a Hokuyo UTM-30LX LASER scanning device that provides horizontal profiles of the surroundings. The disturbance covariance matrix, assumed Gaussian, for the vehicle dependent state variables is defined as $\mathbf{Q}_V = T_s \, \text{diag}\left(\sigma_z^2, \sigma_v^2 \, \mathbf{I}_3, \sigma_{b_r}^2\right)$, with $\sigma_z = 0.04$ m, $\sigma_v = 0.02$ m/s, $\sigma_{b_r} = 5.7 \times 10^{-5}$ deg/s, and the landmark position disturbance covariance matrix is given by $\mathbf{Q}_{\mathbf{p}_i} = T_s \, \sigma_p^2 \, \mathbf{I}_2$, $\sigma_p = 0.07$ m. The altitude measurement is also considered to be zero-mean Gaussian distributed noise with variance $\mathbf{R}_z = \sigma_z^2$, $\sigma_z = 0.03$ m, and the landmark position measurement noise is given as a function of ρ_{i_m} and α_{i_m}, which are the correspondent range-bearing coordinates of the detected landmark $\mathbf{p}_{i_m}$, and also function of the angular and range standard deviation values, $\sigma_\alpha = 3.75$ deg, $\sigma_{\rho_1} = 0.15$ m, and $\sigma_{\rho 2} = 0.25$ m, which can be defined as

$$\mathbf{R}_{\mathbf{p}_{i_m}} = \sigma_{\rho_{i_m}}^2 \, \mathbf{M}_{\alpha_{i_m}} + \sigma_\alpha^2 \, \frac{d\,\mathbf{M}_{\alpha_{i_m}}}{d\alpha}$$

assuming a small angle approximation such that $\mathbf{M}_\alpha = \mathbf{R}_\alpha \, \text{diag}(1, 0) \, \mathbf{R}_\alpha^T$, where $\mathbf{R}_\alpha$ is the 2-D rotation matrix obtained from α. Also, the range measurement noise of the LASER sensor depends on the distance to the detected target, being defined as $\sigma_{\rho_{i_m}} = \sigma_{\rho_1}$ if $\rho_{i_m} \leq 10$ m and as $\sigma_{\rho_{i_m}} = \sigma_{\rho_2}$ if $\rho_{i_m} > 10$ m. Note that the above implicit linearization is just a way to properly approximate the sensor noise and does not influence any of the filter properties.

In sensor-based SLAM, the localization is trivial, as the vehicle is at the origin and aligned with the body frame. As for the mapping, the proposed algorithm provides at each instant a map of the environment with consistent uncertainty estimates. These results are presented in Fig. 1, with a detailed view of the last part of the trajectory shown in Fig. 1(b). It can be seen that in this sensor-based framework, as there is no vehicle localization uncertainty, the unobserved landmarks uncertainty increases, which allows for a consistent map estimation, and eventually to close the loop. The uncertainty of the older landmarks at the right bottom corner of the map, which are deliberately left as duplicates of the new landmarks being detected, would enable the proper association and loop closing procedure for the global sensor-based map. Note that the proposed algorithm provides also

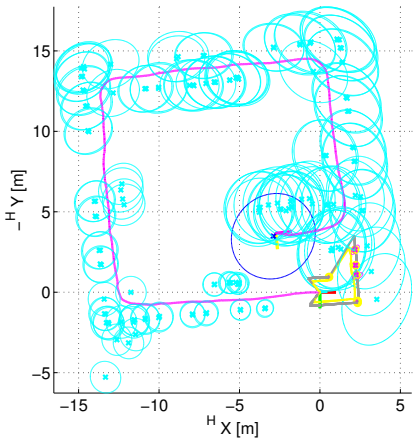

(a) Complete map

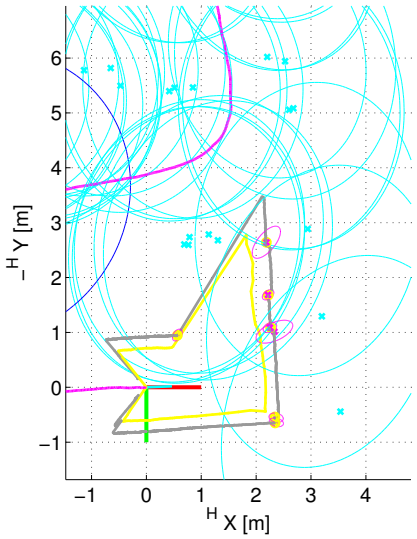

(b) Detailed view

Fig. 1. Map and trajectory in $\{H\}$ frame, featuring the landmark position and 95% confidence bounds, depicted in light blue, and the trajectory of the vehicle, in magenta. The duplicate landmarks, that could be used for loop closure are also depicted in magenta, whereas the current laser profile is depicted in gray and the visibility polygon in yellow.

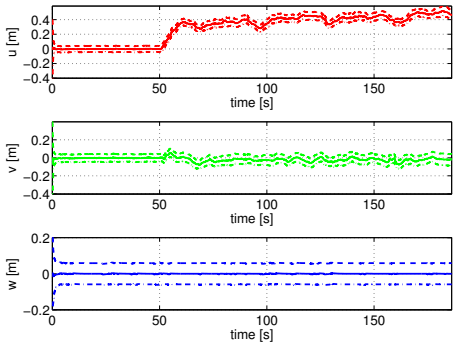

(a) Linear Velocity

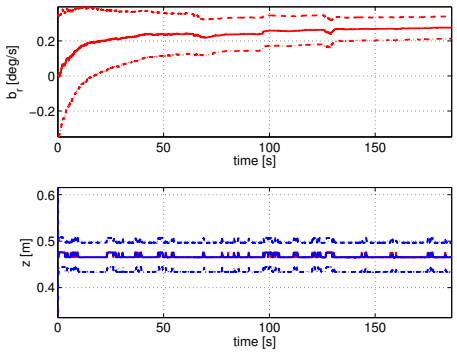

(b) Rate Gyro Bias and Altitude

Fig. 2. Vehicle state time evolution.

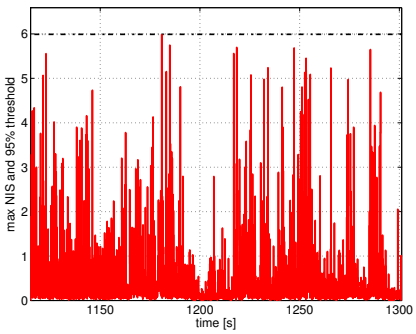

Fig. 3. NIS association maximum (solid red) and $\chi^2_{n_m,95\%}$ threshold (dashed-dotted black).

consistent estimates of the linear motion of the vehicle, shown in Fig. 2, along with the remaining vehicle related variables, without resorting to any odometry sensor, which are not available for aerial vehicles.

Another measure of consistency of the SLAM algorithm when ground truth data is not available, is the maximum normalized innovation squared (NIS) value at each time instant, considering all the landmark associations. This maximum value can be compared, for instance, with the 95% threshold as presented in Fig. 3, that is,

$$\text{NIS}_{i_k} = \boldsymbol{\nu}_{i_k} \mathbf{S}_{i_k}^{-1} \boldsymbol{\nu}_{i_k} \leq \chi^2_{n_m,95\%} \ , \tag{9}$$

where $n_m = \dim(\mathbf{m}_i)$ is the dimension of the landmark position vector. It can be seen that this maximum value seldom approaches the threshold and it is mostly concentrated below $\chi^2_{n_m,5\%}$, which might indicate some degree of conservativeness. In Fig. 4, the evolution of the number of landmarks is provided, and it can be observed that a basic landmark management is done to avoid spurious landmarks due to bad detection.

As there is no vehicle trajectory in this sensor-based SLAM formulation but rather landmark trajectories, the inertial transformations computed in the previous sections are necessary to recover the trajectory of the vehicle as well as the inertial version of the landmark map. As it can be seen in Fig. 1, the trajectory of the vehicle is included for completion of the sensor-based results, by transforming the obtained inertial trajectory into frame $\{H\}$. The inertial map and trajectory computed using both methods, (a) optimization based closed-form solution and (b) state augmentation with open-loop integration, described in Section IV are presented in Fig. 5, whereas the heading of the vehicle is shown in Fig.

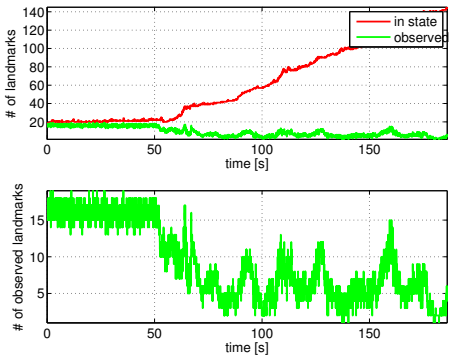

Fig. 4. Total and Observed Number of Landmarks. In the second axis of this figure the number of observed landmarks at each iteration is presented in detail.

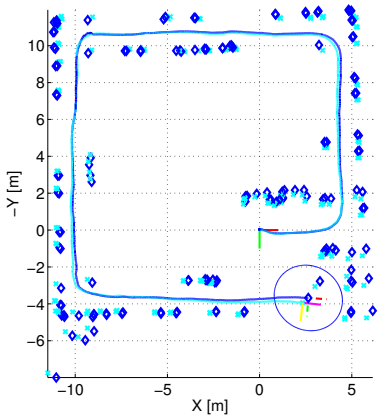

Fig. 5. Map and trajectory in $\{I\}$ frame. The trajectory and map computed using the augmented state approach is represented in dashed dark blue, while the optimization problem approach is shown in light solid blue.

6. It can be seen that both transformations provide coherent results and, notably, that the effects of the magnetic distortions in indoors environments can be devastating, as shown in the latter figure. Note that the heading solution provided by an attitude filter, which uses the IMU magnetometer, is utterly wrong.

VI. Conclusions and Future Work

This paper presents two strategies for the online inertial map and trajectory estimation designed for the sensor-based globally asymptotically stable SLAM filter introduced in the companion paper [1], as well as an indepth analysis of the experimental SLAM results, both in sensor and inertial frames. Conversely to traditional EKF-SLAM algorithms, the proposed SLAM filter avoids depending on the attitude and position representation of the vehicle, yielding globally asymptoticaly stable error dynamics. With the online inertial map and trajectory estimation strategy proposed in this paper the vehicle attitude, position, velocity, and landmark map can be obtained in each filter iteration, with a small computational overhead. The performance and consistency of the proposed SLAM filter and the inertial map and trajectory transformation are evaluated in a structured real world environment. The algorithm produces a consistent map

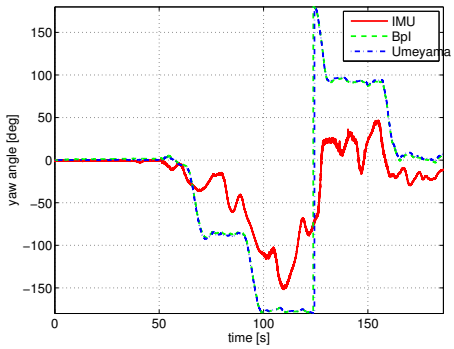

Fig. 6. Heading of the vehicle relative to frame I. The heading computed using the augmented state approach is represented in dashed dark blue, while the optimization problem approach is shown in light solid blue. The red line represents the magnetometer-based heading obtained by an external attitude algorithm.

estimation that can be used to close a 60 meter long loop right in the sensor-based map, while still providing very good estimates of the inertial map and trajectory.

Future work includes the computation of the uncertainty estimates related to the transformation from the sensor frame to the inertial frame, allowing a fair comparison between the two strategies presented in the paper.

Acknowledgements

The authors would like to express their gratitude to the DSOR Lab Quadrotor team for providing the ideal platform for data acquisition, which enabled us to experimentally validate the algorithm presented in this paper.

References

[1] B. J. Guerreiro, P. Batista, C. Silvestre, and P. Oliveira, "Sensor-based Simultaneous Localization and Mapping – Part I: GAS Robocentric Filter," in *Proceedings of the 2012 American Control Conference*, June 2012.

[2] H. Durrant-Whyte and T. Bailey, "Simultaneous Localization and Mapping: part I," *Robotics Automation Magazine, IEEE*, vol. 13, no. 2, pp. 99–110, 2006.

[3] T. Bailey and H. Durrant-Whyte, "Simultaneous Localization and Mapping (SLAM): part II," *Robotics Automation Magazine, IEEE*, vol. 13, no. 3, pp. 108–117, 2006.

[4] K. S. Arun, T. S. Huang, and S. D. Blostein, "Least-Squares Fitting of Two 3-D Point Sets," *Pattern Analysis and Machine Intelligence, IEEE Transactions on*, vol. PAMI-9, no. 5, pp. 698–700, sept. 1987.

[5] S. Umeyama, "Least-squares estimation of transformation parameters between two point patterns," *Pattern Analysis and Machine Intelligence, IEEE Transactions on*, vol. 13, no. 4, pp. 376–380, April 1991.

[6] P. Schönemann, "A Generalized Solution of the Orthogonal Procrustes Problem," *Psychometrika*, vol. 31, pp. 1–10, 1966.

[7] P. Batista, C. Silvestre, and P. Oliveira, "Single Range Aided Navigation and Source Localization: observability and filter design," *Systems & Control Letters*, vol. 60, no. 8, pp. 665–673, Aug. 2011.

[8] R. Kalman and R. Bucy, "New Results in Linear Filtering and Prediction Theory," *Transactions of the ASME - Journal of Basic Engineering*, vol. 83, no. 3, pp. 95–108, March 1961.

[9] A. Gelb, *Applied Optimal Estimation*. MIT Press, May 1974.

[10] J. A. Castellanos, R. Martinez-Cantin, J. D. Tardós, and J. Neira, "Robocentric Map Joining: Improving the Consistency of EKF-SLAM," *Robotics and Autonomous Systems*, vol. 55, no. 1, pp. 21–29, January 2007.